2006

Helicase-binding to DnaI exposes a cryptic DNA-binding site during helicase loading in Bacillus subtilis

Charikleia Ioannou
University of Nottingham, hara@uow.edu.au

Patrick M. Schaeffer
Australian National University

Nicholas E. Dixon
University of Wollongong, nickd@uow.edu.au

Panos Soultanas
University of Nottingham

Helicase-binding to DnaI exposes a cryptic DNA-binding site during helicase loading in Bacillus subtilis

Abstract

The Bacillus subtilis DnaI, DnaB and DnaD proteins load the replicative ring helicase DnaC onto DNA during priming of DNA replication. Here we show that DnaI consists of a C-terminal domain (Cd) with ATPase and DNA-binding activities and an N-terminal domain (Nd) that interacts with the replicative ring helicase. A Zn21-binding module mediates the interaction with the helicase and C67, C70 and H84 are involved in the coordination of the Zn21. DnaI binds ATP and exhibits ATPase activity that is not stimulated by ssDNA, because the DNAbinding site on Cd is masked by Nd. The ATPase activity resides on the Cd domain and when detached from the Nd domain, it becomes sensitive to stimulation by ssDNA because its cryptic DNAbinding site is exposed. Therefore, Nd acts as a molecular 'switch' regulating access to the ssDNA binding site on Cd, in response to binding of the helicase. DnaI is sufficient to load the replicative helicase from a complex with six DnaI molecules, so there is no requirement for a dual helicase loader system.

Keywords

binding, dnai, exposes, cryptic, dna, site, during, helicase, loading, subtilis, bacillus, CMMB

Disciplines

Life Sciences | Physical Sciences and Mathematics | Social and Behavioral Sciences

Publication Details

Ioannou, C., Schaeffer, P. M., Dixon, N. E. & Soultanas, P. (2006). Helicase-binding to DnaI exposes a cryptic DNA-binding site during helicase loading in Bacillus subtilis. Nucleic Acids Research, 34 (18), 5247-5258.

Published online 26 September 2006 *Nucleic Acids Research, 2006, Vol. 34, No. 18* ***5247–5258***
doi:10.1093/nar/gkl690

Helicase binding to DnaI exposes a cryptic DNA-binding site during helicase loading in *Bacillus subtilis*

Charikleia Ioannou, Patrick M. Schaeffer[1], Nicholas E. Dixon[1] and Panos Soultanas*

Centre for Biomolecular Sciences, School of Chemistry, University of Nottingham, University Park, Nottingham NG7 2RD, UK and [1]Research School of Chemistry, Australian National University, Canberra ACT 0200, Australia

Received June 13, 2006; Revised September 4, 2006; Accepted September 7, 2006

ABSTRACT

The *Bacillus subtilis* DnaI, DnaB and DnaD proteins load the replicative ring helicase DnaC onto DNA during priming of DNA replication. Here we show that DnaI consists of a C-terminal domain (Cd) with ATPase and DNA-binding activities and an N-terminal domain (Nd) that interacts with the replicative ring helicase. A Zn^{2+}-binding module mediates the interaction with the helicase and C67, C70 and H84 are involved in the coordination of the Zn^{2+}. DnaI binds ATP and exhibits ATPase activity that is not stimulated by ssDNA, because the DNA-binding site on Cd is masked by Nd. The ATPase activity resides on the Cd domain and when detached from the Nd domain, it becomes sensitive to stimulation by ssDNA because its cryptic DNA-binding site is exposed. Therefore, Nd acts as a molecular 'switch' regulating access to the ssDNA binding site on Cd, in response to binding of the helicase. DnaI is sufficient to load the replicative helicase from a complex with six DnaI molecules, so there is no requirement for a dual helicase loader system.

INTRODUCTION

Bacterial chromosome replication initiates at an origin (*oriC*) where the ubiquitous origin recognition protein DnaA binds to begin the recruitment of the replisome (1,2). The initial step of this process involves the coordinated assembly of a primosome to load the main replicative ring helicase and then recruit the primase (3,4). Successful assembly of the primosome allows the synthesis of primers and recruitment of the DNA polymerase III holoenzyme for elongation to begin. Occasionally replication forks collapse and different restart mechanisms reassemble the replisome at sites other than *oriC*, depending on the structure of the arrested fork. In *Escherichia coli* the PriA/PriB/DnaT dependent mechanism restarts the replisome when a 3′ end is available whilst the PriC-dependent mechanism is involved when there is a single-strand gap at the fork (5,6).

In *Bacillus subtilis* loading of the ring helicase DnaC (homologue of *E.coli* DnaB, 44% identity) is achieved by the action of three primosomal proteins DnaD, DnaB (not to be confused with the *E.coli* DnaB helicase) and DnaI, (7–9). DnaI is homologous to *E.coli* DnaC (10,11), the helicase loader (12,13); it is not to be confused with the *B.subtilis* DnaC helicase. There are no homologues of DnaD and DnaB in *E.coli* but homologues of both proteins, as well as DnaI, are found in low G+C Gram-positive bacteria (7). DnaI interacts with DnaC (14,15) and together with DnaB loads DnaC onto DNA in a DnaD-dependent manner (16). The precise molecular events that underpin the function of the DnaD-DnaB-DnaI primosomal cascade are not clear but data suggest that DnaD acts early, setting the stage for the recruitment of the DnaI–DnaC complex (17,18), while DnaB may be acting together with DnaI to form a pair of helicase loaders for the recruitment of DnaC (16). Alternatively, DnaB may act as a membrane attachment protein to regulate initiation of DNA replication by regulating the recruitment of DnaD to the membrane (19,20). DnaD interacts with DnaA (17), PriA (18) and DnaB (21), disrupts the helicase–DnaI complex and exhibits a DNA architectural activity similar to the histone-like *E.coli* HU proteins (22–24). DnaB also exhibits a DNA remodelling activity that counteracts that observed for DnaD and the two proteins have been proposed to link nucleoid reorganization and initiation of DNA replication (22,23).

B.subtilis DnaI interacts functionally with the *Bacillus stearothermophilus* DnaB helicase (referred to as stearoDnaB to distinguish it from *B.subtilis* DnaB), altering its ATPase activity profile and stimulating its helicase activity (11). StearoDnaB is highly homologous to the *B.subtilis* DnaC helicase (82% identity and 92% similarity) and is expressed in soluble form in *E.coli*. In the absence of DNA it forms a stable complex with DnaI with an apparent stoichiometry of $stearoDnaB_6$-$DnaI_{1\ or\ 2}$ (11). By comparison, *B.subtilis* DnaC

*To whom correspondence should be addressed. Tel: +44 115 9513525; Fax: +44 115 8468002; Email: panos.soultanas@nottingham.ac.uk

is expressed in insoluble form in *E.coli* but forms a soluble complex with DnaI, with apparent stoichiometry $DnaC_6$-$DnaI_6$ when the two proteins are co-expressed and purified in the presence of ATP (16). Purified DnaC and DnaI proteins do not re-associate to form a homogeneous $DnaC_6$–$DnaI_6$ complex at low μM concentrations even in the presence of ATP, but form instead a variety of complexes with wide ranging stoichiometries at 15 μM in the presence of ATP (16).

Structural information about bacterial helicase loaders is lacking and apart from the presence of Walker A and B motifs, nothing is known about the biochemical properties of DnaI. Here we report that DnaI is a two-domain protein with a 21 kDa C-terminal domain (Cd) that binds DNA and hydrolyses ATP, and a 16 kDa Zn^{2+}-containing N-terminal domain (Nd) that interacts with the replicative helicase. The Zn^{2+}-binding module mediates the interaction with the helicase, with the C67, C70 and H84 residues involved in the coordination of the Zn^{2+}. The fourth Zn^{2+}-coordinating residue is either C76 or C101. DnaI binds MANT-ATP with 1:1 stoichiometry and exhibits ATPase activity under conditions of excess of enzyme over ATP. Our data suggest that Nd masks a cryptic DNA-binding activity that resides on Cd. Therefore, Nd acts as a molecular switch modulated by the binding of the helicase. Surface plasmon resonance (SPR) studies show, that in the presence of ATP, DnaI alone is sufficient to efficiently load the helicase at the 5′ end of immobilized ssDNA, and that only the $stearoDnaB_6$–$DnaI_6$ complex is capable of being loaded. DnaI then dissociates rapidly, followed by much slower dissociation of the helicase. We therefore propose a model for the DnaI-mediated helicase loading in *B.subtilis* that does not require a dual helicase-loader system.

MATERIALS AND METHODS

Limited proteolysis

Limited proteolysis was carried out with subtilisin (1:5000 subtilisin : DnaI molar ratio) at 50 mM Tris (pH 7.4), 1 mM EDTA, 10% v/v glycerol at 37°C. Samples were removed at time intervals and the reaction terminated by addition of loading buffer (1% SDS, 2.5% DTT, 0.1% w/v bromophenol blue and 10% w/v glycerol) prior to SDS–PAGE analysis. A protein fragment from subtilisin proteolysis was identified by N-terminal protein sequencing.

Protein purifications

wtDnaI. DnaI was purified from the wt *dnaI* gene, cloned both in pET28a and pET22b, as described before (11) but with treatment of the cell extract with benzonase.

DnaI mutants

The purification method for the C67A, C70A, C76A, H84A and C101A mutants was the same as for wtDnaI up to the first column, apart from the initial suspension buffer that contained 50 mM glutamate and 50 mM arginine. Mutant proteins were partially soluble (∼30%) and were loaded onto a HiTrap Blue Sepharose column, equilibrated in TD (Soultanas, 2002), 0.1 μM EDTA, and eluted with 2 M NaCl. Fractions were pooled, diluted with TD, 0.1 μM EDTA to 6 mS and applied to a heparin column, equilibrated in TD, 0.1 μM EDTA. Proteins were eluted with a 0–500 mM NaCl gradient. Fractions were pooled, protein precipitated with ammonium sulphate, dissolved in TD, 0.1 μM EDTA, 100 mM NaCl and applied to a Superdex S75 gel filtration column, equilibrated in TD, 0.1 μM EDTA, 100 mM NaCl. Fractions were pooled and the absorbance at 280 nm was measured before being made up to 10% v/v with glycerol and freezing.

The K174A mutant was purified as for the wtDnaI except that it was expressed at 27°C overnight (60% soluble) and collected in the flow-through from the HiTrap Q column.

Nd and Cd domains

His-tagged Nd and Cd were purified using a 5 ml HiTrap His-tag column (Amersham Pharmacia Biotech) loaded with Ni^{2+} or Zn^{2+}, followed by gel filtration in a Superdex S75 column. Both proteins were finally in 50 mM Tris (pH 7.5), 0.1 μM EDTA, 100 mM NaCl, 1 mM DTT, 10% v/v glycerol. A significant fraction of Cd (∼50% as assessed by SDS–PAGE) was found in the insoluble fraction.

StearoDnaB

The stearoDnaB helicase was purified as described before (25).

Circular dichroism (CD)

The spectra were recorded on an Applied Photophysics Pi-Star-180 spectrophotometer at 25°C. The temperature was regulated using a Neslab RTE-300 circulating programmable water bath and a thermoelectric temperature controller (Melcor). The protein samples were prepared at 5 μM, in 50 mM Tris (pH 7.4), 0.1 mM EDTA, 1 mM DTT, 100 mM NaCl, 10% v/v glycerol and recorded using a 1 mm path length cuvette. A background spectrum of just the buffer was also recorded and subtracted from each protein spectrum. Each spectrum was recorded from 280 to 200 nm using a 2 nm step and 4.0 nm entrance and exit slit widths. All mutant proteins were analyzed and compared to the wtDnaI. Molar ellipticities were calculated using the equation $[\theta] = \theta/(10 \times n \times c \times l)$ were θ is ellipticity, n is the number of peptide bonds, c is the molar concentration and l is the path length of the cuvette.

Analytical gel filtration

Purified proteins at 5 μM each (7 μM in the case of the DnaI mutants) in 50 mM Tris (pH 7.5), 0.1 mM EDTA, 1 mM DTT and 100 mM NaCl were incubated for 10 min at room temperature to ensure complex formation. The mixture was applied to a Superdex S200 column (Amersham Pharmacia Biotech) equilibrated in the same buffer. Fractions (0.5 ml) were collected and samples were analysed by SDS–PAGE. StearoDnaB is a stable hexamer (305 kDa) whereas DnaI, Nd and Cd are monomers in solution with molecular weights of 36.1, 16.6 and 21.6 kDa, respectively.

Gel shift assays

Gel shift assays were carried out with DnaI, Nd or Cd at 0.25–28 μM, in the presence or absence of ADPNP or ATP (1 mM) in a buffer containing 20 mM Tris (pH 7.4), 0.1 mM EDTA, 4 mM $MgCl_2$, 1 mM DTT, 10% v/v

glycerol and radiolabelled single-strand oligonucleotides (Supplementary Figure S1) at 2.5 nM, unless otherwise stated (26). Proteins were incubated with the oligonucleotide substrate for 10 min at room temperature and then samples were resolved through an 8% w/v polyacrylamide, 5% v/v glycerol native gel, in 0.5×TBE buffer supplemented with 10 mM $MgCl_2$, at 80 V at room temperature. Gels were dried under vacuum and visualized with a phosphorimager (Molecular Imager FX, Bio-Rad). Supershift assays were carried out in a similar manner using DnaI (8 μM) and increasing concentrations of stearoDnaB (0.25–28 μM).

Yeast two hybrid (Y2H) experiments

Y2H experiments were carried out using the MATCHMAKER Two-Hybrid system 2 (Clontech). The *dnaB* gene was cloned as an NcoI–XhoI fragment in the NcoI–SalI sites of pAS2-1 whereas Nd and Cd were cloned as NcoI–XhoI fragments in the same sites of pACT-2. Quantification of the interactions was carried out by β-galactosidase assays using ONPG (*o*-nitrophenyl β-D-galactopyranoside), as described by Clontech. The positive control is based on the p53-SV40 T antigen interaction, using the pAV3-1 plasmid carrying the GAL4 DNA-binding domain fused to murine p53 and a *trp* nutritional selection marker and the pTD1 plasmid carrying the GAL4 activation domain fused to the SV40 large T antigen and a *leu* nutritional selection marker. The negative control shows that there is no interaction between DnaB and SV40 large T antigen, using the pAS2-1-DnaB and pTD1 plasmids, described above. All plasmids were transformed into yeast by electroporation, as described elsewhere (27) and detection of positive interactions was carried out by the agarose overlay method (28) or the filter-lift method (Clontech).

Atomic absorption spectroscopy

The Zn content of DnaI and Nd was estimated by flame atomic absorption spectroscopy using a Perkin–Elmer atomic absorption spectrophotometer (Model 603) in the air-acetylene flame mode, which gives a lean blue flame for Zn. Measurements were standardized with standard $ZnCl_2$ solutions in the same buffer as the protein The wavelength of the hollow cathode lamp was set at 213.9 nm and proteins were prepared in 50 mM Tris (pH 7.5), 0.1 μM EDTA, 1 mM DTT, 100 mM NaCl. The zero reference was set with buffer in the absence of protein.

The PAR assay

The PAR (4-(2-pyridylazo)resorcinol) assay was carried out as described before (29). Purified DnaI was dialysed in 50 mM Tris (pH 7.5). PAR (100 μM) was added to the protein solution (10 μM) and different aliquots of the DnaI/PAR mixture were then prepared in the presence of increasing concentrations (0.1–1.6 mM) of *p*-chloromercuribenzoic acid (PMBA). The absorbance at 500 nm (A_{500}) was measured for all the aliquots. The Zn^{2+} ions released from DnaI by PMBA were coordinated by PAR and the resulting PAR–Zn^{2+} complex absorbed light at 500 nm with an extinction coefficient of 10^4 M^{-1} cm^{-1}. An increase of A_{500} indicates the release of Zn^{2+} ions from the protein. Increasing concentrations of EDTA were added in the aliquot with the highest concentration of PMBA and the A_{500} was monitored. Gradual decrease in A_{500} indicated the extraction of the metal from the PAR–Zn^{2+} complex by EDTA.

Site-directed mutagenesis

All point mutants were constructed with the QuikChange site-directed mutagenesis kit (Stratagene) using the wild-type *dnaI* gene cloned in pET22B, according to the manufacturer's instructions. The mutagenic oligonucleotides used are shown in Supplementary Figure S1. All mutant genes were sequenced to verify the correct mutation.

Fluorescence studies

Binding of ATP to DnaI and Cd was investigated using *N*-methylanthraniloyl ATP (MANT-ATP), a fluorescent analogue of ATP. Binding reactions were carried out at different concentrations of DnaI (1–50 μM) or Cd and MANT-ATP (90–500 nM) in binding buffer [20 mM Tris (pH 7.5), 5 mM $MgCl_2$, 1 mM EDTA and 10% v/v glycerol), using Starna fluorimeter special optical cells (3 mm path and 315 μl volume) in a total volume of 300 μl. The excitation wavelength was set at 356 nm and fluorescence changes were measured at 440 nm. All binding reactions were carried out in triplicate and each reaction was scanned 10 times to obtain a final average for analysis. Binding stoichiometries were measured by continuous variation binding analysis (30). Both [MANT-ATP] and [DnaI] were varied for a fixed and constant summed concentration of 1.1 μM at room temperature.

Thin layer chromatography (TLC)—based ATPase assays

ATPase activity was assayed by monitoring the ^{32}Pi produced during hydrolysis of [γ-^{32}P]ATP (3000 Ci/mmol) using TLC with TEI plates, under conditions of excess DnaI over ATP. All reactions were carried out at 37°C in triplicate, with different concentrations of [γ-^{32}P]ATP (1.66, 3.33, 8.32, 16.65, 25 and 33.3 nM), 8 μM protein (DnaI, Cd, Nd and K174A) in binding buffer and in the presence or absence of 0.48 mM 33mer single-strand oligonucleotide. Samples were removed at time intervals (0–120 min) and reactions were terminated with the addition of 20 mM EDTA. Small samples (1.2 μl) were spotted onto TLC plates that were then developed in 1 M formic acid, 0.5 M $LiCl_2$ and analysed using a phosphorimager. The percentage conversion of ATP to Pi was used to determine the increase of [Pi] with time.

SPR experiments

Experiments were carried out at 20°C in a BIAcore 2000 at 5 μl/min with HBSEP buffer (Biacore) supplemented with 1 mM DTT as running buffer, essentially as described previously (31). A solution (100 nM) of 3′-biotinylated $(dT)_{35}$ in running buffer was injected over a streptavidin-coated chip surface (Biacore SA chip) to yield an increase of 300 RU (1 min) on one flow cell. Another flow cell was unmodified and served as a control. The binding buffer was HBSP (Biacore) supplemented with 10 mM $MgCl_2$ and 2.7 mM ATP. When required to remove tightly-bound proteins, regeneration of the flow cells was achieved with 1 min injection of 50 mM NaOH/1 M NaCl. StearoDnaB, DnaI and Nd were

diluted in binding buffer and injected in combinations or individually during 1 or 2 min, followed by dissociation in running buffer. The binding buffer was selected because it gave the strongest binding of stearoDnaB-DnaI onto ssDNA. Use of the running buffer (without Mg^{2+}/ATP and with 3 mM EDTA) during the dissociation phase resulted in a fast dissociation of DnaI from the loaded complex, allowing the observation of the subsequent slow dissociation of stearoDnaB from the ssDNA. When the binding buffer was used throughout, the same biphasic dissociation was observed, but with a slower DnaI dissociation phase, making it difficult to determine the stoichiometry of the complex.

RESULTS

DnaI is a two-domain protein

DnaI was sensitive to subtilisin and a cleavage site was identified by N-terminal protein sequencing (data not shown). Subtilisin treatment and N-terminal sequencing identified a domain boundary at the sequence QVDI, separating two domains; Nd 16 644 and Cd 21 619 Da.

Both Nd and Cd were tagged with hexahistidine tags at their C-termini. Nd was over-expressed as soluble protein but Cd was 50% soluble (data not shown). Nd was purified using a 5 ml HiTrap-Ni^{2+}-chelating column and gel filtration through Superdex S75. Attempts to fully solubilize Cd at different temperatures and/or expression inductions at different isopropyl-β-D-thiogalactopyranoside (IPTG) concentrations were unsuccessful (data not shown). Repositioning of the hexahistidine tag at the N-terminus of Cd did not improve solubility. N-terminally tagged Cd was consistently 50% soluble upon expression in large scale cultures (data not shown). It was purified from the soluble fraction in good quantities to carry out its biochemical characterization.

Nd interacts with stearoDnaB

DnaI interacts with stearoDnaB [(11) and Figure 1A] and *B.subtilis* DnaC (16), forming stable complexes that can be isolated by gel filtration. StearoDnaB eluted at ~9.8 ml and DnaI at 14.5 ml. The precise elution volume depends on the actual gel matrix and the size of the particular column, but the resolution power of the Superdex S200 column is not sufficient to clearly separate complexes above 200 kDa in size. However, the clear shift of some DnaI into the earlier peak in the presence of stearoDnaB indicates the formation of a complex (Figure 1A). An interaction between Nd and stearoDnaB could also be detected by gel filtration (Figure 1B). While Nd eluted at ~18.2 ml in the presence of stearoDnaB some Nd appeared in the earlier peak indicating the formation of a complex. The interactions of DnaI and Nd with stearoDnaB were also verified by yeast two hybrid experiments (Figure 2A). By comparison, Cd exhibited a very weak interaction in these experiments (Figure 2B and C) and no complexes with stearoDnaB or Nd were detected by gel filtration (data not shown). These data were confirmed with quantitative ONPG assays (Figure 2B). Several yeast clones carrying Cd were tested and although none exhibited significant DnaB-interactions, weak signals just above the background were detectable (Figure 2B and C).

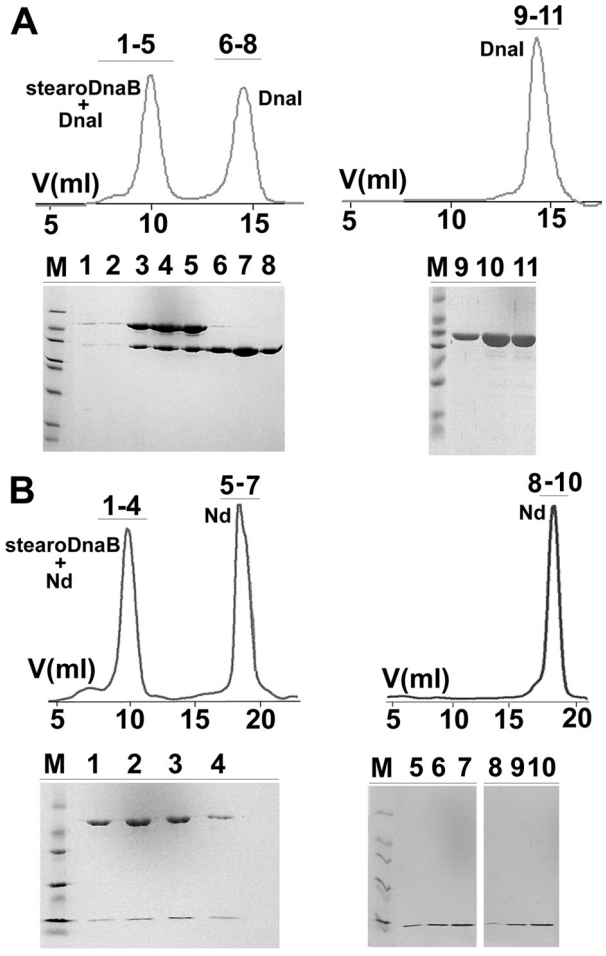

Figure 1. Investigation of the DnaI–stearoDnaB interaction by analytical gel filtration. (**A**) The gel filtration profile of a mixture of DnaI and stearoDnaB (5 μM each) is shown on the left and of the DnaI protein alone on the right. Samples from the peaks were analyzed by SDS–PAGE analysis. The numbers of the lanes in the gels correspond to the areas marked with the same numbers in the elution profiles. The complex is detected in fractions 1–5 in the early peak whilst free DnaI is found in fractions 6–8 and 9–11 in the later peak. (**B**) The same experiment was carried out with Nd and stearoDnaB (5 μM each). The complex is detected in fractions 1–4 in the early peak whereas Nd on its own elutes in the later peak, fractions 5–7 and 8–10.

DnaI binds Zn^{2+}

The C67, C70, C76, H84 and C101 residues in Nd are part of the sequence $CX_2CX_5CX_7HX_{16}C$ that could potentially coordinate Zn^{2+}. The Zn^{2+} contents of DnaI and Nd were investigated by atomic absorption spectroscopy. Four different DnaI preparations, at different concentrations (2.8 and 4.2 μM) were used using standard solutions of Zn^{2+} and the presence of the metal was confirmed (Table 1). The Zn^{2+} molar contents were measured at 1:1 and 1:1.6 relative to the protein. Similar experiments were carried out with Nd but our initial data revealed that it contained less Zn^{2+} than expected, estimated at 1:25.3 relative to the protein (Table 1). One explanation for the poor Zn^{2+} content of Nd could be that the Ni^{2+} column used in our first purification step of the His-tagged Nd may have competed off the Zn^{2+}. We investigated this using a Zn^{2+}-loaded column and a preparation of Nd purified in this manner was assayed for Zn^{2+}.

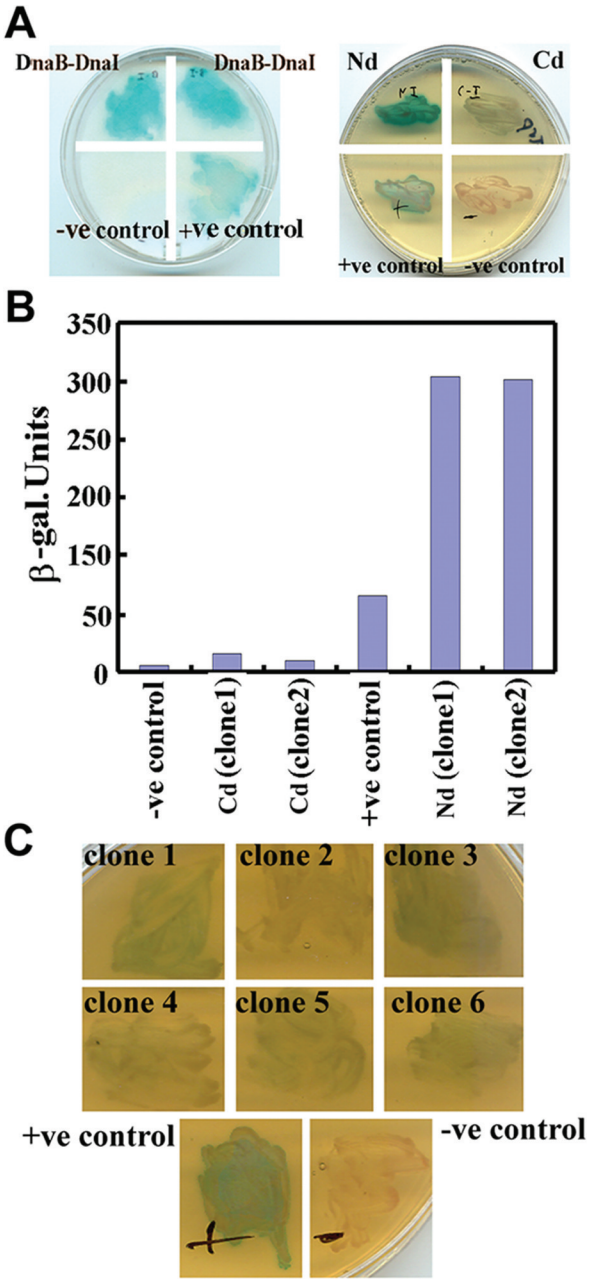

Figure 2. Investigation of the DnaI–stearoDnaB interaction by yeast two hybrid. (**A**)Yeast two hybrid experiments revealed strong interactions between DnaI and stearoDnaB, as well as Nd and stearoDnaB. An interaction between Cd and stearoDnaB could not be detected. (**B**) The Nd–stearoDnaB interaction was verified by ONPG assays. Assays with two different clones each of Nd and Cd are shown. Cd did not reveal an interaction with DnaB. (**C**) Weak interactions between Cd and stearoDnaB were revealed by yeast two hybrid. Six different clones of Cd were tested and they all exhibited weak and variable interactions with stearoDnaB.

The data confirmed the presence of Zn^{2+} in 1:1 molar ratio (Table 1). The involvement of cysteines in Zn^{2+} coordination was established directly using the PAR assay (Supplementary Figure S2). The gradual increase of the absorbance at 500 nm, as *p*-hydroxymercuribenzoic acid was titrated into a solution of DnaI and PAR, indicated the release of Zn^{2+} from cysteines and the formation of the PAR–Zn^{2+} complex. Subsequent titration of increasing concentrations of EDTA resulted in decreasing absorbance indicating the release of Zn^{2+} from PAR and its chelation by EDTA.

Table 1. The Zn content of the Nd and DnaI proteins

Protein	Concentration (μM)	Zn (μM)	Protein:Zn
wtDnaI	2.8	2.9	1:1
	4.2	2.6	1.6:1
Nd_a	19.2	0.8	25.3:1
Nd_b	8.8	9.0	1:1
C67A	4.6	0	0
C70A	1.4	0	0
C76A	2.8	1.7	1.6:1
	8.7	3.1	2.8:1
H84A	0.5	0	0
	5.8	0	0
C101A	3.1	2.3	1.3:1
	1.9	0	0

Nd_a indicates Nd purified through a Ni-loaded His-tag column.
Nd_b indicates Nd purified through a Zn-loaded His-tag column.

A Zn^{2+}-binding module mediates the interaction with the helicase

The C67A, C70A, C76A, H84A and C101A mutants of DnaI were constructed to identify the residues involved in metal coordination. Mutant proteins, when expressed in *E.coli* were partially soluble (~30% soluble; data not shown) and were purified in good quantities for biochemical investigations. Atomic absorption experiments revealed that the C67A, C70A and H84A mutants contained no Zn^{2+}, whereas C76A still bound Zn^{2+} (Table 1). The C101A mutant gave mixed results. In one preparation Zn^{2+} was undetectable but in another Zn^{2+} was detected. We conclude that residues C67, C70 and H84 are involved in Zn^{2+}-binding whereas C76 is not. The status of C101 could not be confirmed unequivocally (see Discussion for an explanation). Notably, all the mutant proteins were partially soluble after sonication of the cells only in the presence of 50 mM glutamate and 50 mM arginine, indicating that these mutations alter somewhat the solubility properties of the protein (32). This is not the result of misfolding as the CD spectra of all mutant proteins were identical to the wtDnaI, indicating similar overall folds (Supplementary Figure S3). In addition, all the mutant proteins eluted at the same point as the wtDnaI through the Superdex S200 gel filtration column indicating proper globular folding.

An intriguing possibility was the involvement of the Zn^{2+}-binding module in interaction with the helicase. This was examined directly using analytical gel filtration. Mutant DnaI proteins were mixed with stearoDnaB in 1:1 molar ratio and the mixtures were resolved through a Superdex S-200 column. Samples from the peaks were analysed with SDS–PAGE (Figure 3). The ability of DnaI to interact with the helicase was dependent upon its ability to bind Zn^{2+}. The C67A and H84A mutants did not interact with the helicase, the C70A mutant exhibited very weak interaction barely detectable by gel filtration, whereas the C76A and C101A mutants retained their ability to interact. These data are consistent with data obtained from the atomic absorption experiments, where the C67A, C70A and H84A proteins were

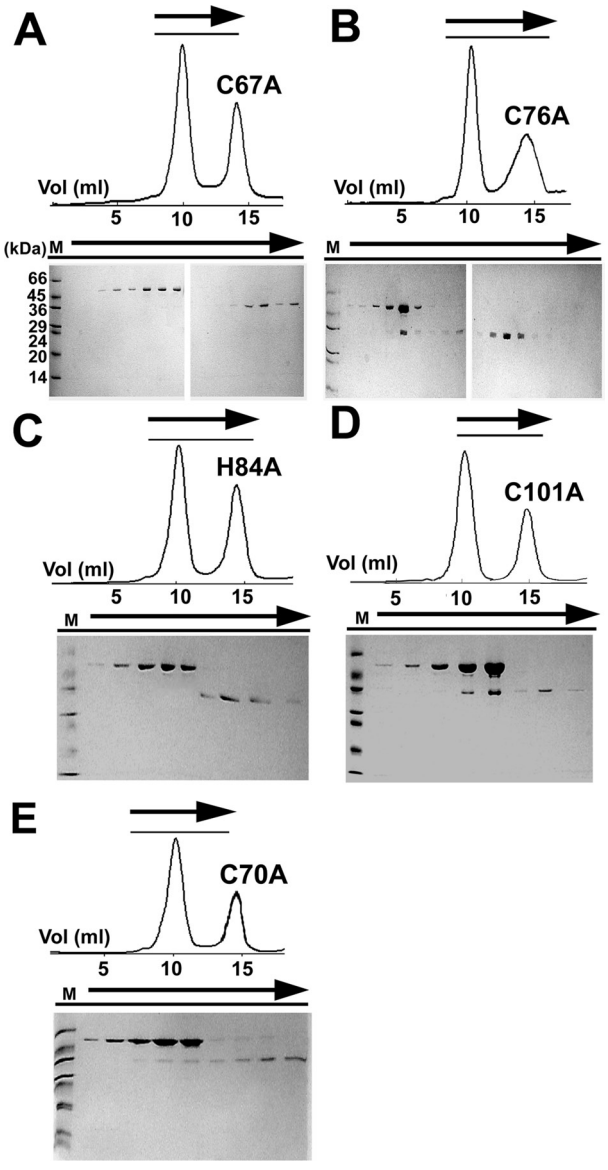

Figure 3. Investigation of the DnaI mutants–stearoDnaB interactions by analytical gel filtration. Gel filtration profiles of DnaI mutants mixed with stearoDnaB are shown. Samples from the peaks indicated by the arrows were analyzed by SDS–PAGE to reveal the identity of the proteins. The masses of the molecular markers are indicated in (A). The stearoDnaB helicase does not form stable complexes with the C67A (**A**) and H84A (**C**) but does form complexes with the C76A (**B**) and C101A (**D**) mutants. The interaction with C70A is considerably weaker (**E**).

unable to bind Zn^{2+}, whereas the C76A protein was able to bind Zn^{2+} and the C101A protein gave mixed results (Table 1).

DnaI binds MANT-ATP in 1:1 stoichiometry

Binding of ATP to DnaI was investigated by fluorescence using MANT-ATP. The binding stoichiometry was determined using the continuous variation analysis from Job plots and the fitted lines gave an intersection at the stoichiometry 1:1 (Figure 4A). Binding was examined at four different [MANT-ATP] (90, 200, 300 and 500 nM) while the [DnaI] was varied and the fluorescence change was plotted

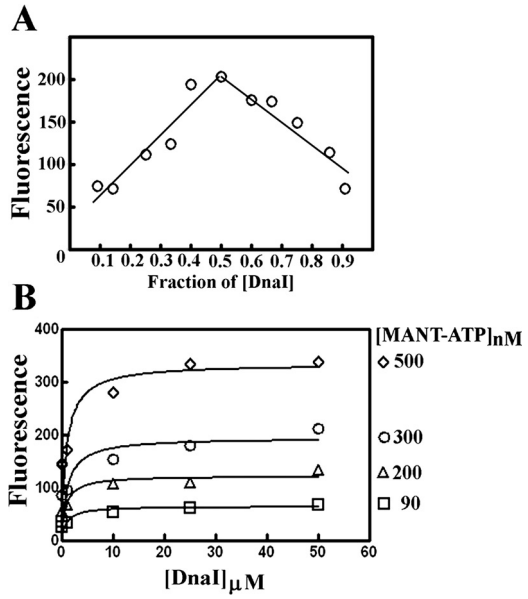

Figure 4. MANT-ATP binding to DnaI. (**A**) A Job plot for MANT-ATP binding to DnaI. The sum of the concentrations of MANT-ATP and DnaI was kept constant at [MANT-ATP] + [DnaI] = 1.1 μM. The fluorescence (arbitrary units) was plotted as a function of the molar fraction of [DnaI] relative to the total ([MANT-ATP] + [DnaI]) concentration. The intersection for the fitted lines gives a value close to 0.5, indicating a binding stoichiometry of MANT-ATP:DnaI of 1:1. (**B**) Determination of the apparent dissociation constant (K_D) for MANT-ATP binding to DnaI. Experiments were carried out at four fixed concentrations of MANT-ATP, as indicated, and the fluorescence (arbitrary units) was plotted as a function of [DnaI]. The data were fitted to a single-site binding hyperbola and analysed by the GraphPad Prism programme to obtain K_D values for each set of data. The dissociation constant is $K_D = 0.9$ μM.

as function of [DnaI], (Figure 4B). The binding curves were fitted to an one site binding hyperbola using GraphPad Prism and K_D values were obtained for each curve (0.89, 0.78, 1.09 and 0.94 μM), indicating an average $K_D = 0.9$ μM for binding of DnaI to MANT-ATP.

DnaI exhibits limited ATPase activity

Although DnaI has Walker A and B motifs and binds ATP, no ATPase activity has been demonstrated to date. The DnaI ATPase activity was demonstrated by TLC assays under conditions of excess protein over ATP, and was found to be unaffected by ssDNA (Figure 5). Since the Walker A and B motifs reside in the Cd domain, its ATPase activity was also examined under the same conditions. Cd exhibited poorer ATPase activity compared to the full-length protein but in the presence of ssDNA, the activity was stimulated to the same level as that of DnaI (Figure 5). By comparison, Nd exhibited no detectable ATPase activity (data not shown), and the Walker A K174A mutant exhibited reduced ATPase activity (Supplementary Figure S4).

Under conditions of excess ATP over protein, DnaI failed to fully hydrolyse all the ATP even after 2 h, indicating that the enzyme does not turn over ATP (Supplementary Figure S5). These data imply that once DnaI hydrolyses ATP it is then locked into an inactive ADP-bound conformation. We also observed that at a fixed ATP concentration (50 μM) all DnaI molecules turn over ATP once (0.1 μM DnaI hydrolyses

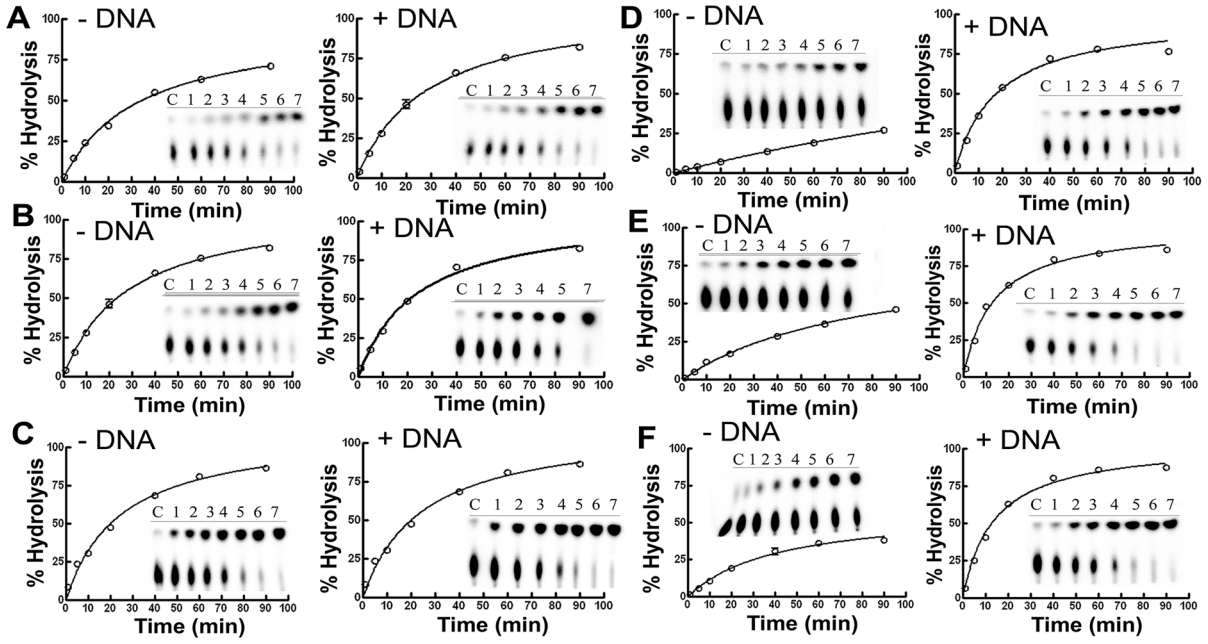

Figure 5. The ATPase activity of DnaI. Conversion of ATP to ADP + Pi by DnaI (**A–C**) and Cd (**D–F**) as a function of time at five different concentrations of [γ-^{32}P]ATP of 1.66, 8.32, 16.65, 25 and 33.3 nM in the presence or absence of ssDNA. Representative TLC plates are shown for experiments carried out with 1.66 nM [γ-^{32}P]ATP (A and D), 16.65 nM [γ-^{32}P]ATP (B and E) and 33.3 nM [γ-^{32}P]ATP (C and F). Reactions were carried out with 8 μM proteins (DnaI or Cd) and in the absence and presence of 480 μM 33mer single-stranded oligonucleotide, as indicated. Lanes marked c indicates control reactions incubated for 120 min in the absence of DnaI. Lanes 1–7 indicate incubation times of 1, 5, 10, 20, 40, 60 and 90 min, respectively. All reactions were carried out in triplicates and the percentage of ATP converted to ADP + Pi was plotted as a function of time, as shown.

0.1 μM ATP) but as the concentration of DnaI is increased the relative fraction of DnaI molecules that hydrolyses ATP is decreased (Supplementary Figure S5). For example, 1, 5, 10, 25 and 50 μM DnaI hydrolyse 0.7, 2.9, 3.9, 8.8 and 14.4 μM ATP, respectively. This may be because as the DnaI concentration is increased not all DnaI molecules have bound ATP or at high DnaI concentrations there may be some kind of regulatory inhibitory effect by DnaI–DnaI interactions or even there may be an ATP-induced oligomer being formed with some DnaI molecules in the oligomer no longer capable of hydrolysing ATP.

A cryptic DNA-binding site is located on the Cd domain

The ssDNA-induced stimulation of Cd ATPase activity implies that this domain binds ssDNA. By comparison, the lack of stimulation of the full-length DnaI in the presence of ssDNA implies that either it does not bind ssDNA or ssDNA binding does not confer the conformational changes required for ATPase stimulation. To distinguish between these two possibilities, the DNA-binding ability of DnaI with single-strand and fork-DNA substrates using gel shift assays was examined (Figure 6A). Under our experimental conditions in the range 0.25–28 μM DnaI-binding to a single-strand 50mer oligonucleotide was undetectable whereas weak binding to fork-substrates was detected (Figure 6A). Binding to ssDNA could only be detected at concentrations higher than 0.9 mM DnaI (data not shown). DnaI exhibited weak binding to 3′- and 5′-tailed DNA substrates (data not shown). The presence of ADPNP or ATP had no effect on DNA binding. Thus, the lack of stimulation of DnaI ATPase activity is a reflection of its inability to bind ssDNA. Instead

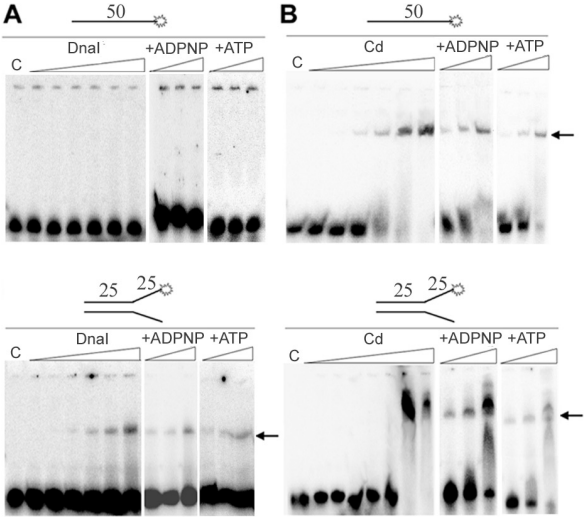

Figure 6. DNA binding gel shift assays. (**A**) Full length DnaI does not bind to ssDNA in the presence or absence of ADPNP or ATP (top) whereas it binds weakly to a fork-DNA substrate (bottom). (**B**) Cd binds to ss (top) and fork (bottom) DNA substrates. In the presence of ADPNP or ATP its DNA binding activity is marginally reduced. DNA substrates are shown on top of the gels. Asterisks indicate the radioactively labelled 5′ end and arrows indicate the shifted bands. Increasing concentrations of DnaI are indicated by sloping bars, left to right 0.25, 0.5, 1, 2, 4 and 8 μM in the absence of ADPNP and 2, 4 and 8 μM in the presence of ADPNP or ATP. Lanes labelled C indicate controls without protein.

it exhibits a preference for ss-dsDNA junctions but binding is still weak.

Similar analysis of Cd revealed that it binds to ssDNA and to fork-substrates (Figure 6B), confirming that the observed

stimulation of its ATPase activity is the result of its interaction with ssDNA. The presence of ADPNP or ATP resulted in a marginal decrease of DNA binding. Therefore in the full-length protein, the Nd domain 'masks' the DNA-binding site on the Cd domain. This cryptic DNA-binding site has been revealed upon Cd detachment from Nd.

The DnaI–stearoDnaB complex binds ssDNA in the presence of ADPNP

Although DnaI binds to stearoDnaB, the stability of the complex is not affected by ADPNP in the absence of DNA (11). In the presence of 1 mM ADPNP stearoDnaB binds better to ssDNA, as shown before (33), whilst in the presence of 8 μM DnaI and increasing concentrations of stearoDnaB (0.25–28 μM) a super-shifted band was detected representing binding of the DnaI–stearoDnaB complex to DNA (compare left and right segments in Figure 7A). DnaI does not bind to ssDNA as shown in Figure 6A. In the absence of ADPNP no super-shifted complex was observed (compare left and right segments in Figure 7B). In the presence of 1 mM ATP the super-shifted band disappeared (Figure 7C). More efficient loading was observed at higher DnaI:stearoDnaB molar ratios, 32:1, 16:1, 8:1 (Figure 7A, lanes 1–3 right segment) compared to lower molar ratios 4:1, 2:1, 1:1 (lanes 4–6), indicating that under these experimental conditions excess of DnaI is required to ensure formation of a stable loading complex. These data indicate that binding of the DnaI–stearoDnaB complex to ssDNA is stimulated by ATP-binding and ATP hydrolysis facilitates the dissociation of the complex leaving the helicase on the DNA.

DnaI is required for efficient loading of stearoDnaB onto ssDNA

An assay for DnaI-mediated loading of stearoDnaB onto ssDNA using SPR (BIAcore) was devised in a similar manner to that described for the interaction between the C-domain of *E.coli* DnaG and *E.coli* DnaB (31). A 3′-biotinylated $(dT)_{35}$ was first loaded onto a streptavidin chip, exposing the 5′ end. Then either stearoDnaB alone or a mixture of stearoDnaB and DnaI were injected, in the presence of Mg-ATP. No interaction of 175 nM stearoDnaB or 1.75 μM DnaI, alone with DNA was observed (Figure 8A; red and light blue). Binding was detected when the two proteins were combined, and the response depended on the concentration of DnaI. Therefore, formation of a complex of DnaI with stearoDnaB is necessary for helicase loading onto ssDNA. The response consistently decreased by 40% over 2 min to a stable value regardless of [DnaI]. The simplest explanation for this behaviour is that the stearoDnaB–DnaI complex first loads, and then one of the components dissociates. We proceeded to discover which component dissociates from the ternary complex.

DnaI dissociates after the helicase is loaded onto ssDNA

The ternary complex was formed by injection of a mixture of stearoDnaB-DnaI (175 nM:1.75 μM). After the fast dissociation phase, the same concentration of DnaI (1.75 μM) alone was injected again and the second binding response indicated re-formation of the ternary complex (Figure 8B; blue). When stearoDnaB was injected instead, very little binding to ssDNA was observed under these conditions, while no binding was apparent on the same flow cell after stearoDnaB was stripped from the ssDNA (data not shown). Therefore, it is the stearoDnaB that remains stably bound to the DNA after dissociation of DnaI and the ternary complex re-forms upon addition of more DnaI.

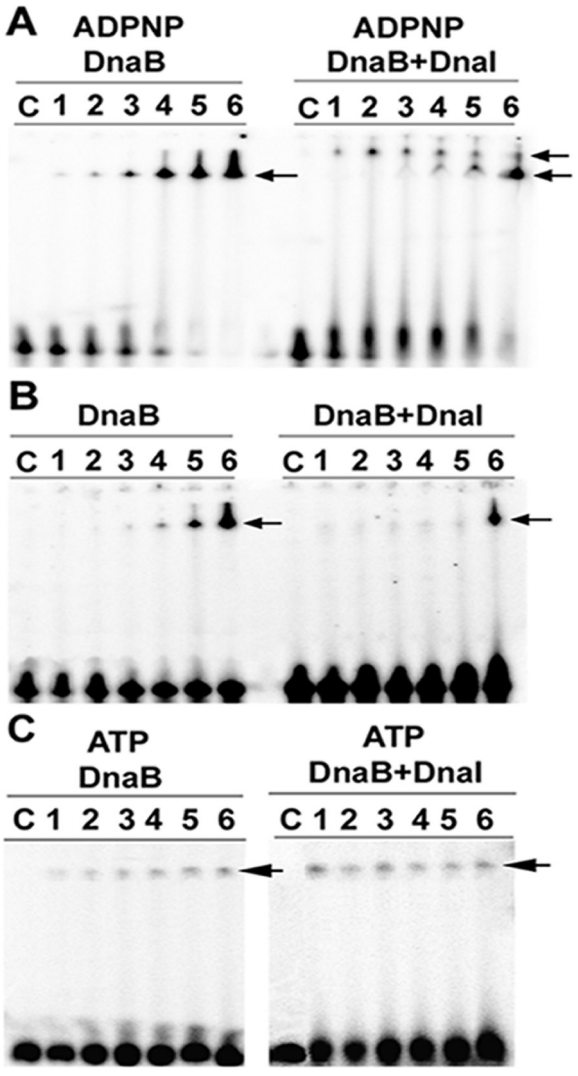

Figure 7. Binding of the helicase loader (DnaI)-helicase (stearoDnaB) complex to ssDNA. Gel shifts showing binding of increasing concentrations of stearoDnaB (lanes 1–6, 0.25, 0.5, 1, 2, 4 and 8 μM, respectively) to a 50mer single-stranded oligonucleotide in the presence of 1 mM ADPNP (**A**), in the absence of ADPNP (**B**), in the presence of 1 mM ATP (**C**) and in the presence (A–C, right segments) of 8 μM DnaI or absence of DnaI (A–C, left segments), as indicated. Arrows indicate the shifted bands.

Stoichiometry of the complex loaded onto ssDNA

The conditions used in this assay permitted visualization of a biphasic dissociation curve with dissociation rates different enough (fast for DnaI, slow for stearoDnaB) to allow extrapolation to zero time of both parts of the response curve to obtain quantitative measures of the amount of stearoDnaB-DnaI loaded and of stearoDnaB remaining after dissociation of DnaI. Determination of the ratio of bound stearoDnaB to

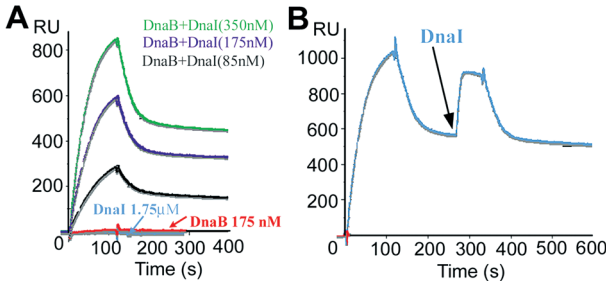

Figure 8. Interaction of the stearoDnaB–DnaI complex with immobilized ssDNA, studied by SPR. (**A**) Investigation of the stearoDnaB–DnaI interaction by SPR. StearoDnaB 175 nM (red) or DnaI 1.75 μM (light blue) shows no binding to the immobilized oligonucleotide (3′-biotinylated dT_{35}). Binding was observed when the two proteins were mixed. Injections of stearoDnaB (175 nM) with increasing amounts of DnaI (black, 85 nM; dark blue, 175 nM; green, 350 nM) exhibited binding responses with a fast dissociation phase. (**B**) DnaI dissociates from the ternary complex in the fast dissociation phase. A mixture of stearoDnaB (175 nM) and DnaI (1.75 μM) shows a biphasic binding response. A second injection of DnaI at 1.75 μM produces a second response, confirming that DnaI can rebind to reform the ternary complex. This shows that it is DnaI that dissociates with a fast off-rate once the stearoDnaB–DnaI complex is loaded on the ssDNA.

total complex loaded showed that for every ratio of components used to generate the data in Figure 8A, the mass ratio was close to 0.6. This corresponds closely to the ratio of masses of the proteins, indicating strict 1:1 stoichiometry of helicase and DnaI in the loaded complex. The high response compared to the ssDNA that is available on the chip, and the well-established properties of hexameric helicases, suggests that it is the hexameric form of the helicase that is loaded, and therefore the only species in the mixture capable of being productively loaded onto the exposed 5′ end of ssDNA was the stearoDnaB$_6$–DnaI$_6$ complex. Complexes with fewer than six molecules of DnaI per helicase hexamer are either not formed in the mixtures because of highly cooperative association of DnaI, or if they are, they are not capable of being loaded at the exposed 5′ end of the ssDNA.

The stearoDnaB$_6$-DnaI$_6$ stoichiometry implied by SPR is different than the apparent stearoDnaB$_6$-DnaI$_{1\ or\ 2}$ stoichiometry implied by gel filtration [(11) and Figure 1]. The latter was deduced based upon the assumption that all of the available stearoDnaB was in complex with DnaI. If this is not true then the peak of the hexameric stearoDnaB will overlap with the peak from the complex and free stearoDnaB will co-elute with the complex, thus giving an apparent impression of less DnaI in the complex. It is indeed difficult to assess the precise stoichiometry of this complex by gel filtration since the resolution power of Superdex S200 is not enough to separate clearly complexes above 200 kDa in size. Also, there appear to be some variability in the stoichiometry of this complex. For example, *B.subtilis* DnaC and DnaI form mainly a DnaC$_6$–DnaI$_6$ complex, when they are co-expressed and co-purified but other complexes with fewer than six DnaI molecules are also apparent (16). When the two proteins are separated and mixed, again they appear to form complexes with fewer than six DnaI molecules per DnaC hexamer (16). In addition, the effect of DNA on the stoichiometry of the complex has not been assessed and one possibility may be that in the presence of ssDNA the stearoDnaB$_6$–DnaI$_6$ complex is more stable.

Not surprisingly, we have been unable to find conditions where the Nd domain of DnaI is capable of loading stearo-DnaB onto ssDNA in these SPR assays. One reason is that it lacks the cryptic DNA-binding region in the Cd domain. Another is that it probably lacks regions in the Cd required for cooperative interactions with the helicase.

DISCUSSION

DnaI interacts with the helicase via its Nd domain

DnaI is the putative helicase loader in *B.subtilis* but the helicase loading mechanism is still unknown. Our data show that DnaI consists of an Nd domain that contains a Zn^{2+}-binding module involved in the interaction with the helicase, and a Cd domain with ATPase and DNA binding activities. However, a very weak interaction between Cd and the helicase was also detected only by yeast two hybrid. Quantification of this weak interaction with six different Cd clones revealed that it is variable. Some clones exhibited slightly better signal than others did, albeit they were all just above the negative control levels. The functional significance of this observation is not clear but it could be argued that a secondary patch that interacts weakly with the helicase resides on Cd. One could speculate that cooperativity in binding of multiple DnaI molecules to the helicase hexamer may also involve protein–protein interactions within or between Cd domains. In the analogous *E.coli* DnaC helicase loader, a single point mutation near the N-terminus also abolished binding to the helicase whilst retaining its ability to bind ATP (34).

DnaI has a cryptic DNA-binding site on its Cd domain

We were unable to detect significant binding of DnaI to ssDNA even at high concentrations in the presence or absence of ADPNP, suggesting that the native protein does not bind ssDNA. Weak binding to fork and tail (5′ or 3′) DNA substrates was detected indicating a slight preference for ds-ssDNA junctions. The weak nature of this interaction makes its biological significance uncertain. Cd exhibited DNA-binding activity. The simplest interpretation of these data is that the Nd domain masks the DNA-binding site located on Cd. Nd acts as a 'molecular switch' that regulates the availability of the DNA-binding site. In the native protein, this site is buried but when the helicase binds to Nd a conformational change reveals the cryptic DNA-binding site. The helicase-loader can now deliver the helicase to the DNA but it can do so only when bound to ATP. This is consistent with the inability of the stearoDnaB–DnaI complex to produce a super-shifted complex on ssDNA in the absence of the ATP analogue ADPNP. Having eliminated misfolding problems, the partial insolubility of Cd is likely to indicate that certain hydrophobic patches on its surface are protected by the presence of Nd in the intact protein and exposed in its absence. It is likely that this allosteric control of domain movement in DnaI is an important functional property regulating helicase loading. Taking into account the combined data, we propose a model for the DnaI-mediated helicase loading (Figure 9). By comparison, the Gram-negative *E.coli* helicase loader DnaC has been reported to exhibit a cryptic ssDNA binding activity only when bound to the

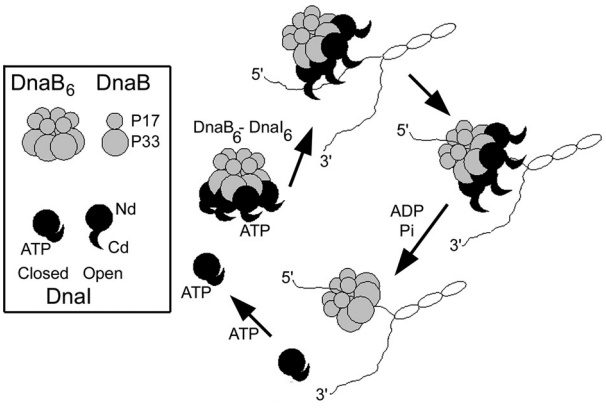

Figure 9. A model for DnaI-mediated helicase loading in *Bacillus*. StearoDnaB consists of two domains, an Nd P17 and a Cd P33, while DnaI consists of an Nd and a Cd, as indicated. DnaI binds ATP in its Cd domain and exists in a 'closed conformation'. The P33 domain of stearoDnaB interacts with the Nd domain of DnaI (11) and a conformational change switches DnaI into a DNA-interacting mode. The cryptic DNA binding site is exposed and the complex binds to the 5′-ssDNA tail. The ATPase activity is stimulated and ATP hydrolysis facilitates the ejection of DnaI from the complex leaving stearoDnaB bound to the DNA.

helicase (35) and to interact weakly to ssDNA in the absence of the helicase, with ATP strengthening this interaction (36). The Cd domain belongs to the AAA family of a diverse group of ATPases (37). They often consist of a non-ATPase Nd that acts in substrate recognition (in our case Nd that recognizes the helicase), followed by one or two AAA domains (in our case the Cd domain). This family also belongs to the classic AAA^+ superfamily of chaperone-like ATPases that assist in the assembly and disassembly of protein complexes and the remodelling of protein–DNA complexes (38).

B.subtilis DnaI has weak ATPase activity

Despite the presence of Walker A and B motifs characteristic of ATP-metabolising enzymes (39) no ATPase activity has been demonstrated for DnaI. Our data reveal that DnaI binds ATP in a 1:1 stoichiometry and hydrolyses ATP. ATP appears to be essential for the formation of a $DnaC_6$–$DnaI_6$ complex when the two proteins are co-expressed and purified from *E.coli* (16) but in its absence complexes of different stoichiometry $DnaB_6$-$DnaI_{1\ or\ 2}$ also have been observed with the stearoDnaB protein (homologous to *B.subtilis* DnaC). Interestingly, the $DnaC_6$–$DnaI_6$ complex cannot be fully reconstituted with purified DnaC and DnaI proteins (16). In the *E.coli* DnaC helicase loader, ATP has been reported to be essential for the formation of a stable helicase loader-helicase complex and binds only to one of two DnaC protein conformations that exist prior to nucleotide binding (12,13,40,41). ATP-binding induces conformational changes that increase its affinity for the helicase, whilst ADP-binding acts as a negative effector. In a similar manner, ATP-binding may also modulate the DnaI conformation thus increasing its affinity for the helicase *in vivo*, although no such effect has been detected *in vitro*. However, the non-hydrolysable analogue ADPNP is able to promote binding of the helicase loader (DnaI)-helicase (stearoDnaB) complex to DNA (Figure 7).

The importance of the ATP-binding site for the conformation of DnaI is highlighted by the effect of the K174A mutation. This mutation affected the solubility of the protein but its CD spectrum and behaviour through gel filtration are identical to wtDnaI, indicating no problems with overall folding. In addition, it retains some ATPase activity suggesting that altering residues in the active site can affect subtly the ATP-binding pocket and ATPase activity. The fact that K174A has reduced ATPase activity compared to wtDnaI indicates that this residue is not directly involved in catalysis, but could be participating along with other residues in ATP-binding. In other ATPases, the effect of mutating the equivalent lysine also appears to have variable consequences. For example, in the F_1F_o-ATPase β-subunit, the K to N/E mutation causes only a 3- to 5-fold reduction in ATPase activity (42) and an equivalent mutation in UvrA causes only a 2-fold decrease in k_{cat} (43), while the K405S mutation in NS-1 of the minute virus of the mouse (MVM) results in a mutant protein with 87% of the ATPase activity of the wild-type protein (44). In the PcrA helicase, the equivalent K37A mutation produces a protein with reduced k_{cat} but tighter K_m retaining reasonable levels of helicase activity (45). Therefore, it is not clear whether the conserved lysine residue of the Walker A motif is involved in nucleotide binding or hydrolysis or in both activities collectively or alternatively in coupling the ATPase reactions with other activities. In contrast, the equivalent K112R mutation in the putative Walker A GKN motif of *E.coli* DnaC produced a soluble protein that was defective in ATP hydrolysis (36). The ATP-binding site in *E.coli* DnaC includes the recognition of many structural elements of the ATP, including the base, ribose, β and γ phosphate groups and these complex interactions may couple ATP-induced conformational changes to allosteric sites elsewhere in the protein (46). *E.coli* DnaC does not hydrolyse ATP but in the presence of an ATPase-dead DnaB mutant or ssDNA, it turns over ATP at 0.6 min^{-1} and 0.9 min^{-1}, respectively. Maximal activity of 3.5 min^{-1} is observed in the presence of both the mutant DnaB and ssDNA (36). Our data indicate that in *B.subtilis*, ATP-binding promotes the association of the helicase loader–helicase complex with DNA and the ATPase activity of DnaI is stimulated upon binding to DNA. ATP hydrolysis promotes the dissociation of the complex leaving the helicase bound to the DNA (Figure 9). Therefore, a single helicase-loader (DnaI) is sufficient to load the hexameric helicase onto the DNA and there is no absolute requirement for a dual helicase loader system as has been suggested before (16).

The role of the Zn^{2+}-binding module

A comparison with DnaI proteins from other species reveals that the Zn^{2+}-binding module is not strictly conserved. *Streptococcus*, *Listeria* and *Enterococcus* proteins have no obvious Zn^{2+}-binding residues. *Staphylococcus* and *Oceanobacillus iheyensis* proteins have $HX_3HX_4CX_6H$ and $CX_2CX_5CX_7S$ sequences, respectively, that could potentially coordinate Zn^{2+}. Even in other *Bacillus* strains, the Zn^{2+}-binding motif is not strictly conserved. For example, the *Bacillus haloduranS* protein has the sequence $CX_2CX_5CX_7Q$ that could also coordinate Zn^{2+}. The C67, C70 and H84 residues are involved in Zn^{2+} coordination but the status of C76 and C101 could not be established unequivocally. A plausible explanation may be that while mutations in the C67, C70

and H84 residues abolish Zn^{2+}-binding, mutations in the C76 and C101 residues may cause local structural rearrangements, thus allowing C101 to substitute C76 for Zn^{2+}-binding in the C76A mutant and vice versa. The compromised ability of the C67A, C70A and H84A proteins to interact with the helicase suggest that the role of the Zn^{2+}-module is to provide the structural framework for this interaction. The biological significance of the apparent structural plasticity of the Zn^{2+}-module and its poor conservation will need further investigation.

SUPPLEMENTARY DATA

Supplementary Data are available at NAR Online.

ACKNOWLEDGEMENTS

The authors thank Dr Laurence Gardiner for help with proteolysis and yeast two hybrid analyses, Karin Loscha for preparation of some protein samples and Graham Balkwill for help with the CD experiments. This work was supported by a BBSRC grant (BB/C500579/1) to P.S., and the Australian Research Council (N.E.D.). Funding to pay the Open Access publication charges for this article was provided by the BBSRC.

Conflict of interest statement. None declared.

REFERENCES

1. Erzberger,J.P., Pirruccello,M.M. and Berger,J.M. (2002) The structure of bacterial DnaA: implications for general mechanisms underlying DNA replication initiation. *EMBO J.*, **21**, 4763–4773.
2. Messer,W. (2002) The bacterial replication initiator DnaA. DnaA and oriC, the bacterial mode to initiate DNA replication. *FEMS Microbiol. Rev.*, **26**, 355–374.
3. Funnell,B.E., Baker,T.A. and Kornberg,A. (1987) *In vitro* assembly of a prepriming complex at the origin of the *E.coli* chromosome. *J. Biol. Chem.*, **262**, 10327–10334.
4. Fang,L., Davey,M.J. and O'Donnell,M. (1999) Replisome assembly at oriC, the replication origin of *E.coli*, reveals an explanation for initiation sites outside an origin. *Mol. Cell*, **4**, 541–553.
5. Sandler,S.J. (2000) Multiple genetic pathways for restarting DNA replication forks in *E.coli* K-12. *Genetics*, **55**, 487–497.
6. Heller,R.C. and Marians,K.J. (2005) The disposition of nascent strands at stalled replication forks dictates the pathway of replisome loading during restart. *Mol. Cell*, **17**, 733–743.
7. Lemon,K.P., Moriya,S., Ogasawara,N. and Grossman,A.D. (2002) Chromosome replication and segregation. In Sonenshein,A.L., Hoch,J.A. and Iosick,R. (eds), *Bacillus subtilis and its closest relatives: From genes to cells*. ASM Press, Washington DC, pp. 73–86.
8. Bruand,C., Ehrlich,S.D. and Jannière,L. (1995) Primosome assembly site in *B. subtilis*. *EMBO J.*, **14**, 2642–2650.
9. Bruand,C., Farache,M., McGovern,S., Ehrlich,S.D. and Polard,P. (2001) DnaB, DnaD and DnaI proteins are components of the *B. subtilis* replication restart primosome. *Mol. Microbiol.*, **42**, 245–255.
10. Koonin,E.V. (1992) DnaC protein contains a modified ATP-binding motif and belongs to a novel family of ATPases including also DnaA. *Nucleic Acids Res.*, **20**, 1997.
11. Soultanas,P. (2002) A functional interaction between the putative primosomal protein DnaI and the main replicative DNA helicase DnaB in *Bacillus*. *Nucleic Acids Res.*, **30**, 966–974.
12. Wahle,E., Lasken,R.S. and Kornberg,A. (1989) The DnaB–DnaC replication protein complex of *Escherichia coli*. I. Formation and properties. *J. Biol. Chem.*, **264**, 2463–2468.
13. Wahle,E., Lasken,R.S. and Kornberg,A. (1989) The DnaB-DnaC replication protein complex of *Escherichia coli*. II. Role of the complex in mobilizing DnaB functions. *J. Biol. Chem.*, **264**, 2469–2475.
14. Imai,Y., Ogasawara,N., Ishigo-Oka,D., Kadoya,R., Daito,T. and Moriya,S. (2000) Subcellular localization of Dna-initiation proteins of *B.subtilis*: evidence that chromosome replication begins at either edge of the nucleoids. *Mol. Microbiol.*, **36**, 1037–1048.
15. Noirot-Gros,M.F., Dervyn,E., Wu,L.J., Mervelet,P., Errington,J., Ehrlich,S.D. and Noirot,P. (2002) An expanded view of bacterial DNA replication. *Proc. Natl Acad. Sci. USA*, **99**, 8342–8347.
16. Velten,M., McGovern,S., Marsin,S., Ehrlich,S.D., Noirot,P. and Pollard,P. (2003) A two-protein strategy for the functional loading of a cellular replicative DNA helicase. *Mol. Cell*, **11**, 1009–1020.
17. Ishigo-Oka,D., Ogasawara,N. and Moriya,S. (2001) DnaD protein of *B.subtilis* interacts with DnaA, the initiator protein of replication. *J. Bacteriol.*, **183**, 2148–2150.
18. Marsin,S., McGovern,S., Ehrlich,S.D., Bruand,C. and Polard,P. (2001) Early steps of *B.subtilis* primosome assembly. *J. Biol. Chem.*, **276**, 45818–45825.
19. Hoshino,T., McKenzie,T., Schmidt,S., Tanaka,T. and Sueoka,N. (1987) Nucleotide sequence of B. subtilis dnaB: a gene essential for DNA replication initiation and membrane attachment. *Proc. Natl Acad. Sci. USA*, **84**, 653–657.
20. Rokop,M.E., Auchtung,J.M. and Grossman,A.D. (2004) Control of DNA replication initiation by recruitment of an essential initiation protein to the membrane of *B.subtilis*. *Mol. Microbiol.*, **52**, 1757–1767.
21. Bruand,C., Velten,M., McGovern,S., Marsin,S., Serena,C., Ehrlich,S.D. and Polard,P. (2005) Functional interplay between the *B.subtilis* DnaD and DnaB proteins essential for initiation and re-initiation of DNA replication. *Mol. Microbiol.*, **55**, 1138–1150.
22. Turner,I.J., Scott,D., Allen,S., Roberts,C.J. and Soultanas,P. (2004) The *B.subtilis* DnaD protein: a putative link between DNA remodelling and initiation of DNA replication. *FEBS Lett.*, **577**, 460–464.
23. Zhang,W., Carneiro,M.J.V.M., Turner,I.J., Allen,S., Roberts,C.J. and Soultanas,P. (2005) The *B.subtilis* DnaD and DnaB proteins exhibit different DNA remodelling activities. *J. Mol. Biol.*, **351**, 66–75.
24. Carneiro,M.J.V.M., Zhang,W., Ioannou,C., Scott,D.J., Allen,S., Roberts,C.J. and Soultanas,P. (2006) The DNA-remodelling activity of DnaD is the sum of oligomerisation and DNA-binding activities on separate domains. *Mol. Microbiol.*, **60**, 917–924.
25. Bird,L.E. and Wigley,D.B. (1999) The *B. stearothermophilus* replicative helicase: cloning, overexpression and activity. *Biochim. Biophys. Acta*, **1444**, 424–428.
26. Soultanas,P., Dillingham,M.S., Papadopoulos,F., Phillips,S.E.V., Thomas,C.D. and Wigley,D.B. (1999) Plasmid replication initiator protein RepD increases the processivity of PcrA DNA helicase. *Nucleic Acids Res.*, **27**, 1421–1428.
27. Becker,D.M. and Guarente,L. (1991) High-efficiency transformation of yeast by electroporation. *Meth. Enzymol.*, **194**, 182–187.
28. Dumay,H., Rubbi,L., Sentenac,A. and Marck,C. (1999) Interaction between yeast RNA polymerase III and transcription factor TFIIIC via ABC10α and τ131 subunits. *J. Biol. Chem.*, **274**, 33462–33468.
29. Hunt,J.B., Neese,S.H. and Ginsburg,A. (1985) The use of 4-(2-pyridylazo)resorcinol in studies of Zinc release from *E.coli* aspartate transcarbamoylase. *Anal. Biochem.*, **146**, 150–157.
30. Lohman,T.M. and Mascotti,D.P. (1992) Nonspecific ligand-DNA equilibrium binding parameters determined by fluorescence methods. *Meth. Enzymol.*, **212**, 424–458.
31. Oakley,A.J., Loscha,K.V., Schaeffer,P.M., Liepinsh,E., Pintacuda,G., Wilce,M.C.J., Otting,G. and Dixon,N.E. (2005) Crystal and solution structures of the helicase-binding domain of *E.coli* primase. *J. Biol. Chem.*, **280**, 11495–11504.
32. Golovanov,A.P., Hautbergue,G.M., Wilson,S.A. and Lian,L.Y. (2004) A simple method for improving protein solubility and long term stability. *J. Amer. Chem. Soc.*, **126**, 8933–8939.
33. Soultanas,P. and Wigley,D.B. (2002) Site-directed mutagenesis reveals roles for conserved amino acid residues in the hexameric DNA helicase DnaB from *B. stearothermophilus*. *Nucleic Acids Res.*, **30**, 4051–4060.
34. Ludlam,A., McNatt,M.W., Carr,K.M. and Kaguni,J.M. (2001) Essential amino acids of *E.coli* DnaC protein in an N-terminal domain interact with DnaB helicase. *J. Biol. Chem.*, **29**, 27345–27353.
35. Learn,B.A., Um,S.-J., Huang,L. and McMacken,R. (1997) Cryptic single-stranded-DNA binding activities of the phage λ P and *E.coli* DnaC replication initiation proteins facilitate the transfer of *E.coli* DnaB helicase onto DNA. *Proc. Natl Acad. Sci. USA*, **94**, 1154–1159.
36. Davey,M.J., Fang,L., McInerney,P., Georgescu,R.E. and O'Donnell,M. (2002) The DnaC helicase loader is a dual ATP/ADP switch protein. *EMBO J.*, **21**, 3148–3159.

37. Patel,S. and Latterich,M. (1998) The AAA team: related ATPases with diverse functions. *Trends Cell Biol*., **8**, 65–71.
38. Neuwald,A.F., Aravind,L., Spouge,J.L. and Koonin,E.V. (1999) AAA+: a class of chaperone-like ATPases associated with the assembly, operation and disassembly of protein complexes. *Genome Res*., **9**, 27–43.
39. Walker,J.E., Saraste,M., Runswick,M.J. and Gray,N.J. (1982) Distantly related sequences in the α and β subunits of ATP synthase, myosin, kinases and other ATP requiring enzymes and a common nucleotide binding fold. *EMBO J*., **1**, 945–951.
40. Galletto,G. and Bujalowski,W. (2002) The *E.coli* replication factor DnaC protein exists in two conformations with different nucleotide binding capabilities. I. Determination of the binding mechanism using ATP and ADP fluorescent analogues. *Biochemistry*, **41**, 8907–8920.
41. Galletto,G. and Bujalowski,W. (2002) Kinetics of the *E.coli* replication factor DnaC protein-nucleotide interactions. II. Fluorescence anisotropy and transient, dynamic quenching stopped-flow studies of the reaction intermediates. *Biochemistry*, **41**, 8921–8934.
42. Parsonage,D., Al-Shawi,M.K. and Senior,A.E. (1988) Directed mutations of strongly conserved lysine 155 in the catalytic nucleotide-binding domain of β-subunit of F1-ATPase from *E.coli*. *J. Biol. Chem*., **263**, 4740–4744.
43. Myles,G.M., Hearst,J.E. and Sancar,A. (1991) Site-specific mutagenesis of conserved residues within Walker A and B sequences of *E.coli* UvrA protein. *Biochemistry*, **30**, 3824–3834.
44. Brosh,R.M. and Matson,S.W. (1995) Mutations in motif II of *E*.coli DNA helicase II render the enzyme non-functional in both mismatch repair and excision repair with differential effects on the unwinding reaction. *J. Bacteriol*., **177**, 5612–5621.
45. Soultanas,P., Dillingham,M.S., Velankar,S.S. and Wigley,D.B. (1999) DNA binding mediates conformational changes and metal ion coordination in the active site of PcrA helicase. *J. Mol. Biol*., **290**, 137–148.
46. Galletto,G., Surendran,R. and Bujalowski,W. (2000) Interactions of nucleotide cofactors with the *E.coli* replication factor DnaC protein. *Biochemistry*, **39**, 12959–12969.